

Evaluation of the solubility of the salt forming ashes from electrostatic precipitators during leaching assays

Authors: Daniel Moreira Saturnino*, Éder Domingos de Oliveira* and Marcelo Cardoso*

Keywords: Pulp and Paper Plants, Recovery Boiler, Electrostatic Precipitator, Leaching and Chloride and Potassium

ABSTRACT

Previous studies indicate that the leaching of the electrostatic precipitator ash is the simplest and one of more economically competitive technique for the removal of alkali soluble non-process elements of the pulp industry. According to the literature, it is possible to remove quantities that vary from 75% to 100% of the chloride and potassium salts from the electrostatic precipitator ashes, with a loss of sodium carbonate and sulphate between 10% and 30%. The use of this technique has been evaluated for many pulp and paper mills around the world. Following this tendency, this study has the focus on obtaining solubility experimental data of the salts present in the ash through leaching tests, in determining the solubilities of these salts using a thermodynamic model and so comparing the experimental data with the results calculated by the thermodynamic model. Based on the phase

diagrams and on solubility curves plotted using the model, it can be determined not only the salts in the solid phase but also the amount removed of each ion (chloride, potassium, carbonate, sodium and sulphate) in the system. Comparing the removal of the ions predicted by the model with those observed in the leaching tests, it has been possible to verify a good agreement (percentual variation not higher than 15%) between the expected values and the experimental ones. Finally, with the purpose of checking the ash behaviour, it was made a X-ray diffraction analysis in the solid phase formed during the leaching tests, which has showed the presence of the same compounds predicted by the model.

INTRODUCTION

Nowadays, the pulp and paper mills (kraft process), like many other chemical industries have faced more strict environmental regulations, which conducted them to intensify the efforts to keep the product quality as well as the production cost with a minimum environmental impact. In this context, a closed-cycle operation is

the key point, i.e., the material recycling is increased and the process effluents are reduced, Ricketts (1994). In the specific case of the pulp and paper industry, which has a relatively closed-cycle production system, another closed-loop addition will generate a higher accumulation of the non-process elements or NPEs (ions chloride, potassium, calcium, magnesium, aluminum, silicon, etc.), mainly, at the black liquor recovery unit, Jemaa et al (1999).

It is reported in the literature many techniques used by some mills to reduce the levels of NPEs. Among them those related to the removal of chloride and potassium from black liquor recovery unit are extensively discussed. The main technologies are based on the evaporation/crystallization of the white liquor and on the treatment of the ash collected by the electrostatic precipitator of recovery boilers. There are many technically and economically feasible processes described in the literature with emphasis to the leaching experiments, Jemaa et al (2000) and Ferreira et al (2003).

According to the literature, the

Authors' references:

*Departamento de Engenharia Química/Escola de Engenharia - eder@deq.ufmg.br
Universidade Federal de Minas Gerais (UFMG) - mcardoso@deq.ufmg.br

leaching process can reach a removal in the range from 75% to 100% of chloride and potassium compounds of electrostatic precipitator ashes from the recovery boiler, with a loss not superior to 10% and 30% of sodium sulphate and sodium carbonate, respectively, Pryke et al (1983) and Minday et al (1998). These losses can be minimized, practically eliminated, through the introduction of a crystallizing operation after the leaching stage. Many industries around the world have evaluated this technique since the 1970's.

This work has the objective to analyze the solubility of the salts that compose the electrostatic precipitator ash during leaching assays with water. In the ash leaching process, it is desired that the maximum quantity of the chloride and potassium compounds be dissolved while the compounds of sodium, sulphate and carbonate stay in the solid phase. So, it is possible to recover these three elements that are important on preparing the white liquor.

Thus, this study is divided in the following steps: (i) acquisition of the solubility experimental data of the salts forming the ash through leaching experiments; (ii) calculation of the solubility data of the salts by a thermodynamic model and (iii) comparison between the experimental data points with those predicted by the theory.

THEORY

There are many thermodynamic models of phase equilibria that predict the salt solubility in a liquid phase and these models try to solve the problem studied here, Malmberg (2002). The model used in this work was originally developed by Gilbert (1976) to describe the phase aspects of the aqueous chemical system: $\text{Na}^+ - \text{K}^+ - \text{Cl}^- - \text{CO}_3^{2-} - \text{SO}_4^{2-} - \text{S}^{2-} - \text{OH}^-$. In the moment, the empiric model developed by Gilbert is the only capable to determine the solubility of the salts present in the

ashes collected by the electrostatic precipitator from the recovery boiler (Saturnini, 2003).

The equation used consists of a third grade polynomial expression which contains the independent parameters: temperature, alkalinity (hydroxide plus sulfide concentration in equivalent gram per litre) and potassium molar ratio in relation to cations $[\text{K}/(\text{K}+\text{Na})]$; as well as, compound parameters which include the concentrations of other compounds in solution. The layout of the equations and the values of the coefficients in the model were determined using stepwise multiple regression statistical techniques. The equations generated were fitted to 3450 solubility experimental data points, Gilbert (1976).

Starting from this model, some changes were made to become possible to apply the original proposed equations to the aqueous system: $\text{Na}^+ - \text{K}^+ - \text{Cl}^- - \text{CO}_3^{2-} - \text{SO}_4^{2-}$, studied in our leaching process. Using the equations, it was possible to plot solubility curves for the system studied; therefore, obtaining the composition of the solid and liquid phases. The data showed in Table 1, placed in a correct way in the Equation 1, will generate the solubility curve for chloride, carbonate and sulphate. After this, comparisons between the results predicted by the model and the experimental data from the leaching tests were made.

$$\begin{aligned}
 Y = & a + b \cdot \text{K}/(\text{K}+\text{Na}) + c \cdot T + \\
 & d \cdot [\text{CO}_3] + e \cdot [\text{Cl}] + f \cdot [\text{K}/(\text{K}+\text{Na})]^2 + \\
 & g \cdot [\text{K}/(\text{K}+\text{Na})] \cdot T + h \cdot [\text{K}/ \\
 & (\text{K}+\text{Na})] \cdot [\text{CO}_3] + i \cdot [\text{K}/ \\
 & (\text{K}+\text{Na})] \cdot [\text{Cl}] + j \cdot [\text{SO}_4] + \\
 & k \cdot T \cdot [\text{CO}_3] + l \cdot T \cdot [\text{SO}_4] + m \cdot [\text{K}/ \\
 & (\text{K}+\text{Na})]^3 + n \cdot [\text{K}/(\text{K}+\text{Na})]^2 \cdot T + \\
 & o \cdot [\text{K}/(\text{K}+\text{Na})]^2 \cdot [\text{CO}_3] + p \cdot [\text{K}/ \\
 & (\text{K}+\text{Na})] \cdot [\text{Cl}] + q \cdot [\text{K}/(\text{K}+\text{Na})] \cdot T^2 + \\
 & r \cdot [\text{K}/(\text{K}+\text{Na})] \cdot [\text{CO}_3]^2 + s \cdot [\text{K}/ \\
 & (\text{K}+\text{Na})] \cdot [\text{Cl}]^2 + t \cdot T^2 \cdot [\text{CO}_3] + \\
 & u \cdot T^2 \cdot [\text{SO}_4] + v \cdot T \cdot [\text{SO}_4]^2
 \end{aligned}
 \tag{1}$$

SOLID PHASE

Figure 1 presents the compounds in the precipitated solid phase in function of the potassium content (expressed by the molar ratio: $[\text{K}/(\text{K}+\text{Na})]$) and the alkali level in the system (expressed by the OH^- molal concentration). These parameters were chosen because the molar ratio is an index that measures the potassium enrichment, while the hydroxide concentration is an important parameter for the white liquor. It is important to state that the alkali level of the leaching system was around zero ($10^{-5} < [\text{OH}^-] < 10^{-4}$), i.e., near the "x" axis.

The diagram showed in Figure 1 describes the equilibrium that exists in the solid phase of the system: $\text{Na}^+ - \text{K}^+ - \text{Cl}^- - \text{CO}_3^{2-} - \text{SO}_4^{2-}$. For example, it can be seen that there is a curve with losangle marks for the equilibrium of the chloride compounds. It must be noticed that on the left of this curve the stable solid phase corresponds to sodium chloride (NaCl). Thus, ash with potassium molar ratio $[\text{K}/(\text{K}+\text{Na})]$ located in this area will have chloride crystallization in sodium chloride form, if the solubility limit of this ion is reached after the mixture of ash and water during the leaching process. On the right side of the curve, the chloride will crystallize as potassium chloride (KCl). Mixtures in which the value of the ratio $[\text{K}/(\text{K}+\text{Na})]$ is located over the curve will show crystallization of both salts.

Considering the phase equilibrium showed by the sulphate (Figure 1), it can be observed two transition curves and four possible solid phases: burkeite ($2\text{Na}_2\text{SO}_4 \cdot \text{Na}_2\text{CO}_3$), sodium sulphate (Na_2SO_4), glasserite ($3\text{K}_2\text{SO}_4 \cdot \text{Na}_2\text{SO}_4$) and potassium sulphate (K_2SO_4). The first transition curve (square marks) divides the diagram in a region where exists sodium sulphate and burkeite simultaneously and other region where the glasserite exists. So, on the left side of this cur-

Table 1 - Coefficients for the solubility curve

Coefficientes	Cloreto (Cl ⁻)	Carbonato (CO ₃ ²⁻)	Sulfato (SO ₄ ²⁻)
a	6,06	3,83	0,457
b	3,97	5,54	0
c	0,00489	0	0
d	-1,08	0	0
e	0	-0,421	0
f	2,66	-10,4	0
g	0	-0,0298	0
h	0,0727	0	-0,00321
i	0	0	0,233
j	-0,00000145	0,000000708	0
k	0	0,000141	0
l	0	0,000086	0
m	0	11,2	0
n	0,0566	0,0613	0
o	0	0	0,465
p	0	-0,565	0
q	0,000000124	0	0,00000477
r	0	0	-0,0606
s	0	0	-0,0303
t	0,000038	0	0
u	0	0,000000469	0
v	0	0,0000000243	0

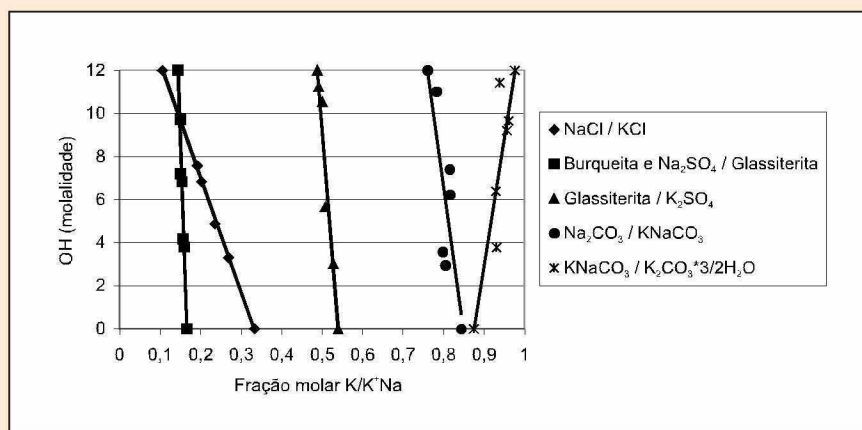


Figure 1 - Solid phase diagram of the system Na⁺ - K⁺ - Cl⁻ - CO₃²⁻ - SO₄²⁻ at 55°C.

ve the sulphate can crystallize like sodium sulphate or burkeite, while, at the right side of the curve, is the region where the glasserite is stable. If the potassium level is very high it is possible to occur another transition indicated by the second curve (tri-

ngle marks) and the sulphate can crystallize as potassium sulphate.

Finally, the phase diagram shows for carbonate three transition curves and four possible solid phases: burkeite (2Na₂SO₄*Na₂CO₃), sodium carbonate (Na₂CO₃), sodium and po-

tassium carbonate (KNaCO₃) and potassium carbonate hydrate (K₂CO₃*3/2 H₂O). On the left side of the first transition curve (square marks), the burkeite crystallization occurs. Between this curve and second one (circle marks) the carbonate will crystallize as sodium carbonate. The crystallization of sodium and potassium carbonate (KNaCO₃) occurs in the region where the potassium molar ratio is located between the second and third transition curve (cross marks). Finally, in the region on the right side of this curve, there is the crystallization of potassium carbonate hydrate.

Once all solid phases are identified, it is possible to determine the solubility curves for the ions that exists in the studied leaching systems.

Liquid phase

Once the solid phase diagram is determined and the regions where each solid compound are established, the next step is the quantitative determination of the ion concentration in the liquid phase. This parameter will be obtained from the solubility curves of the system: Na⁺ - K⁺ - Cl⁻ - CO₃²⁻ - SO₄²⁻ for which we consider the concentration of each anion (Cl⁻ - CO₃²⁻ - SO₄²⁻) versus the cation molar ratio represented by [K/(K+Na)]. With this information, it is also possible, through a mass balance, to determine the solid phase content and also find the removal of each ion. After these data be calculated, it will be possible to compare them with the experimental results. It is expected that the model will be able to help in understanding the behaviour observed. It is also important to say that the solubility curves of each anion will be given in function of the cations molar ratio [K/(K+Na)] in a value of OH⁻ concentration near zero. It will be generated solubility curves for each evaluated temperature in the leaching tests.

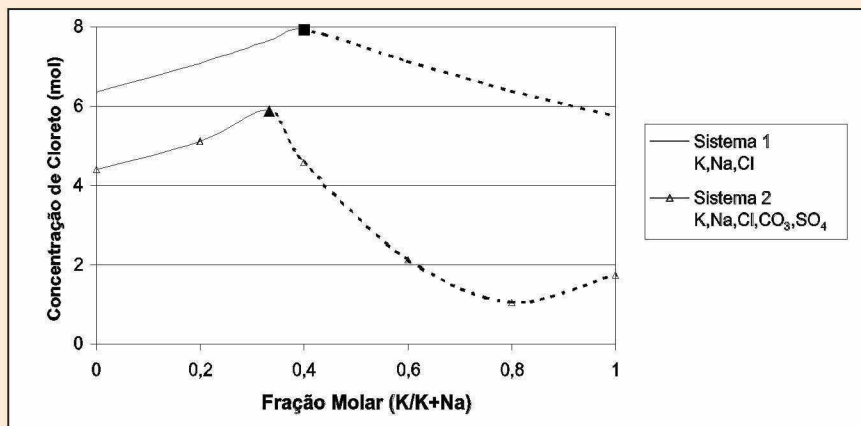


Figure 2 - Chloride solubility curve of the system $\text{Na}^+ - \text{K}^+ - \text{Cl}^- - \text{CO}_3^{2-} - \text{SO}_4^{2-}$ at 55°C .

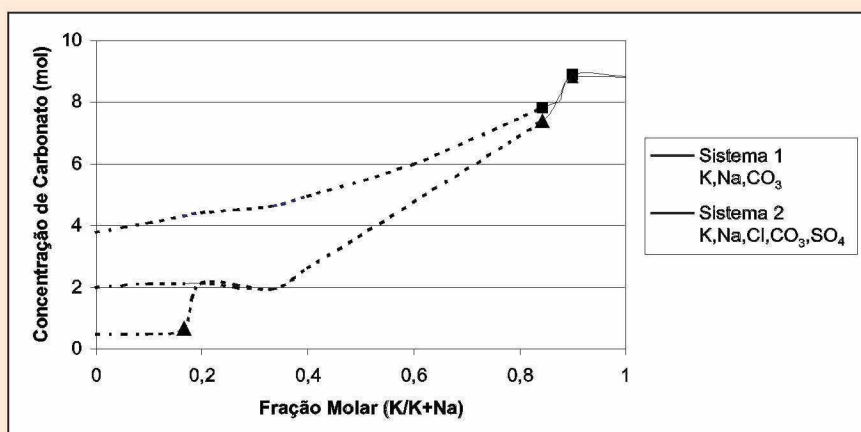


Figure 3 - Carbonate solubility curve of the system $\text{Na}^+ - \text{K}^+ - \text{Cl}^- - \text{CO}_3^{2-} - \text{SO}_4^{2-}$ at 55°C .

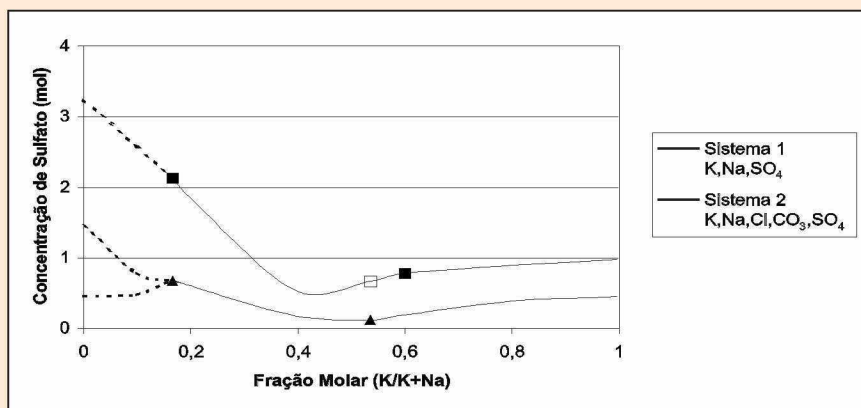


Figure 4 - Sulphate solubility curve of the system $\text{Na}^+ - \text{K}^+ - \text{Cl}^- - \text{CO}_3^{2-} - \text{SO}_4^{2-}$ at 55°C .

In the Figure 2, it is shown the chloride solubility curve at 55°C . In this curve, it is important to notice a specific point (triangle mark) in which the potassium molar ratio $[\text{K}/(\text{K}+\text{Na})]$ assumes the value of 0,333. This point denotes the transition of the sys-

tem from NaCl (continuous line) to KCl (dashed line). Thus, once the chloride concentration reaches values over the chloride solubility curve, it will crystallize as NaCl (if the potassium molar ratio $[\text{K}/(\text{K}+\text{Na})]$ is less than 0,333) or like KCl (if the potassium

molar ratio $[\text{K}/(\text{K}+\text{Na})]$ were greater than 0,333). If the chloride concentration is under the solubility curve, it will be completely dissolved in the liquid phase. Therefore, we have a qualitative and quantitative description of the chloride in both phases.

Solubility curves for carbonate and sulphate versus potassium molar ratio $[\text{K}/(\text{K}+\text{Na})]$ for each temperature were also obtained. Figures 3 and 4 show this solubility curves at 55°C , respectively.

The carbonate solubility curve at 55°C (Figure 3) shows three transition points (triangle marks): the first one is the transition from burkeite ($2\text{Na}_2\text{SO}_4 \cdot \text{Na}_2\text{CO}_3$) to sodium carbonate (Na_2CO_3) at the potassium molar ratio $[\text{K}/(\text{K}+\text{Na})]$ of 0,166. It is important to notice that the presence of two curves in this region is related to the relative concentration of sulphate and carbonate, i.e., initially if the carbonate concentration is higher than the inferior curve, burkeite will crystallize until the sulphate anion is depleted (in this case there is an excess of carbonate). If the carbonate concentration is higher than the superior curve, the remaining carbonate will crystallize as sodium carbonate. On the right side of the first point, only occurs the crystallization of sodium carbonate, so the two curves join in a single one. So, the dashed line represents the region where burkeite and sodium carbonate can crystallize. A second transition point is located at the potassium molar ratio of 0,843 and it refers to the transition from sodium carbonate to sodium and potassium carbonate (KNaCO_3). This region is indicated by a plain continuous line. Finally, the third point, at 0,875, indicates the last transition from sodium and potassium carbonate (KNaCO_3) to hydrated potassium carbonate ($\text{K}_2\text{CO}_3 \cdot 3/2\text{H}_2\text{O}$). This region is represented by a bulk continuous line.

In Figure 4, it is shown the sulphate solubility curve at 55°C , from

which it is possible to observe two transition points (triangle marks) the first one, at potassium molar ratio of 0,166, establishes the region of burkeite crystallization. The two curves on the left side of the first point represent the solubility limit for burkeite (inferior curve) and for sodium sulphate (superior curve). A similar analysis to that previously made for carbonate anion can explain the presence of these two curves. Thus, if the sulphate concentration is higher than that of the inferior curve the burkeite will crystallize and, in the case where the sulphate concentration is higher than the superior curve the sodium sulphate will also crystallize. Between the potassium molar ratio values of 0,166 and 0,539, glasserite ($3K_2SO_4 \cdot Na_2SO_4$) crystallization occurs and, finally, on the right side of the second point ($[K/(K+Na)] = 0,539$) potassium sulphate will crystallize. It is important to mention that in other temperatures the curves show similar profiles, but different concentration values.

METHODOLOGY

Initially, in order to obtain the experimental data, a synthetic ash similar to that studied by Jaretun and Aly (1998) was prepared with the intention to verify the results as well as confirm our experimental set-up and the chemical analysis employed. The synthetic ash was obtained from a mixture of established quantities of salts (sodium chloride, sodium carbonate, sodium sulphate and potassium chloride), at the same composition like that used by Jaretun and Aly (1998). Samples of ashes were also collected from a recovery boiler electrostatic precipitator of a Brazilian mill. The composition of each ash is showed in Table 2.

The leaching tests were realized in a glass reactor inside a controlled water bath. Table 3 shows the leaching

Table 2 - Composition of synthetic and industrial ashes

Elements	Synthetic and studied by Jaretun e Aly (% mass)	Industrial unit (% mass)
Sodium	33,11	29,08
Potassium	1,79	10,13
Chloride	19,24	17,93
Carbonate	3,04	3,82
Sulphate	42,82	39,04
Total	100,00	100,00

parameters studied. All experiments were made in 15 minutes, once this time is sufficient to the phase equilibria be reached in the system. The ash was previously heated to simulate better the real conditions in a mill. The temperature of the system was monitored as well as the mixer's speed (300 r.p.m.) was maintained during the experiment. Once the system reached equilibrium, the mixture was filtered and samples of the solution and solids were collected and submitted to chemical analysis.

The chemical analysis consisted in atomic absorption spectrophotometry for determination of potassium and sodium concentrations; titration with silver nitrate for chloride concentration and titration with hydrochloric acid for carbonate concentration. The sulphate concentration was determined by mass balance and molecular absorption spectrophotometry. The analysis performed by Jaretun and Aly (1998) were ionic chromatography to determine the concentrations of chloride, carbonate and sulphate and plasma emission spectrophotometry to determine the potassium and sodium concentration. The solid phase collec-

ted from the experiments were analysed by x-ray diffraction. Afterwards, comparisons with the results predicted by the thermodynamic model were performed.

RESULTS

In the first series of experiments, synthetic ashes were employed with the purpose to verify the results presented by Jaretun and Aly (1998), as well as to check the experimental layout and the chemical analysis employed. After this procedure, it were performed experiments with ash samples from a mill. The results are shown in Table 3.

Comparing the results obtained from the synthetic ash experiments with those studied by Jaretun and Aly (1998), it can be observed that there is a similarity in the results for the ion extraction (chloride, potassium, carbonate, sodium and sulphate), which generates curves with similar behaviour, but they are slightly different in the extraction values. Specifically for the carbonate, for instance, there is a reduction of the extraction following an increase in temperature and ash concentration, these

Table 3 - Values of each parameter for the ash leaching process

Temperature (°C)	Concentration (kg/l)
55	0,6
65	1,0
75	1,4

Table 4 - Extraction ranges of the ions potassium, chloride, carbonate, sulphate e sodium of the synthetic ash, studied by Jaretun and Aly and industrial.

Extracted Ions	Extraction range for Jaretun and Aly ash (%)	Extraction range for synthetic ash (%)	Extraction range for industrial ash (%)
Potassium	90 - 100	93 - 100	26 - 74
Chloride	75 - 100	65 - 90	65 - 90
Carbonate	85 - 100	60 - 90	5 - 10
Sulphate	10 - 50	18 - 53	5 - 35
Sodium	34 - 70	34 - 70	30 - 60

Table 5 - Potassium molar ratio [K/(K+Na)] of the synthetic and industrial ashes

	Synthetic ash and studied by Jaretun and Aly	Industrial ash
[K/(K+Na)]	0,0265	0,1704

results agree with the tendencies found in Jaretun and Aly work. However, in this work the minimum solubilization of carbonate was nearby 60%, while in literature was 85%. The high percentage of potassium extraction observed, always superior to 90%, for all experiments with synthetic ash, also agree with literature. Comparing the results for the chloride extraction, it has been possible to notice that there are a few differences in the values, probably due to experimental errors, but the

tendency is the same found in the literature. High solubilization of this ion was observed in our experiments (extraction range from 65% to 90%) as well as in Jaretun and Aly work (from 75% to 100%). The results related to sodium extraction agree with that found by Jaretun and Aly, whose extraction values are located in a range between 34% and 70%. For sulphate extraction, the results obtained (18 to 53%) were a little different from those published (10% to 50%). These differences can be ex-

plained by experimental errors during the chemical analysis employed. While the analysis used by Jaretun and Aly (1998) were ionic chromatography and plasma emission spectrophotometry, titration and atomic absorption spectrophotometry were used in this work.

Once it has been checked the extraction ranges for each ion in the ash, the next step consists in to evaluate the results obtained in the leaching process. To analyze these results, the extraction ranges are compared the those calculated using the thermodynamic model. Initially, the potassium molar ratio [K/(K+Na)] was determined for the ash. The results are shown in Table 5.

Based upon the values of the potassium molar ratio [K/(K+Na)] and the solid phase diagram (Figure 1), it

Table 6 - Extraction ranges for potassium in each ash evaluated

	Jaretun e Aly	Synthetic	Industrial ash
Experimental extraction range	90% - 100%	93% - 100%	26% - 74%
Predicted extraction range	100%	100%	27% - 67%

Table 7 - Extraction ranges for the ions: chloride, carbonate, sulphate and sodium for synthetic and Jaretun and Aly ashes.

Ions	Extraction range predicted (%)	Extraction range of Jaretun and Aly (%)	Extraction range of synthetic ash (%)
Chloride	65 - 100	75 - 100	65 - 90
Carbonate	70 - 100	85 - 100	60 - 90
Sulphate	17 - 50	10 - 50	18 - 53
Sodium	37 - 70	34 - 70	34 - 70

has been possible to determine if potassium salts will crystallize. In this way, the model can predict if the potassium will be completely dissolved or not. In Table 6 it is presented the experimental extraction range results and those predicted by the model.

The results for the synthetic ash of this work and that studied by Jaretun and Aly (1998), indicate the inexistence of potassium salts. Therefore, considering this fact, it can be predicted that the potassium extraction will be 100%, or under non ideal conditions a value nearby 100%. It is important to mention that only six points, out of eighteen, for both ashes were different of 100%. These points were obtained in experiments with high ash concentration where it is more difficult to have homogeneous conditions. For the industrial ash, the point with potassium molar ratio equal to 0,1704 is located (Figure 1) where occurs the transition from burkeite ($2\text{Na}_2\text{SO}_4 \cdot \text{Na}_2\text{CO}_3$) to glasserite ($3\text{K}_2\text{SO}_4 \cdot \text{Na}_2\text{SO}_4$). Thus, the potassium molar extraction will be inferior to 100%. It can be observed for this system that the model and the experimental values are in agreement for the potassium extraction. The results of leaching assays can also be observed in Figures 5, 6 and 7.

From the results on Table 4 and Figures 2 to 4, it can be verified that the chloride will crystallize as sodium chloride (NaCl) from all ashes. The sulphate crystallizes as sodium sulphate (Na_2SO_4) from the synthetic ash and glasserite ($3\text{K}_2\text{SO}_4 \cdot \text{Na}_2\text{SO}_4$) from the industrial ash. The carbonate as burkeite ($2\text{Na}_2\text{SO}_4 \cdot \text{Na}_2\text{CO}_3$) from the synthetic ash and sodium carbonate (Na_2CO_3) from the industrial ash. It is important to remember that the crystallization occurs only if the solubility limit of the ion is surpassed. Finally, with the intention to certificate the behaviour described, X-rays diffraction analysis were made in the solid phases formed in the leaching processes. The compounds so-

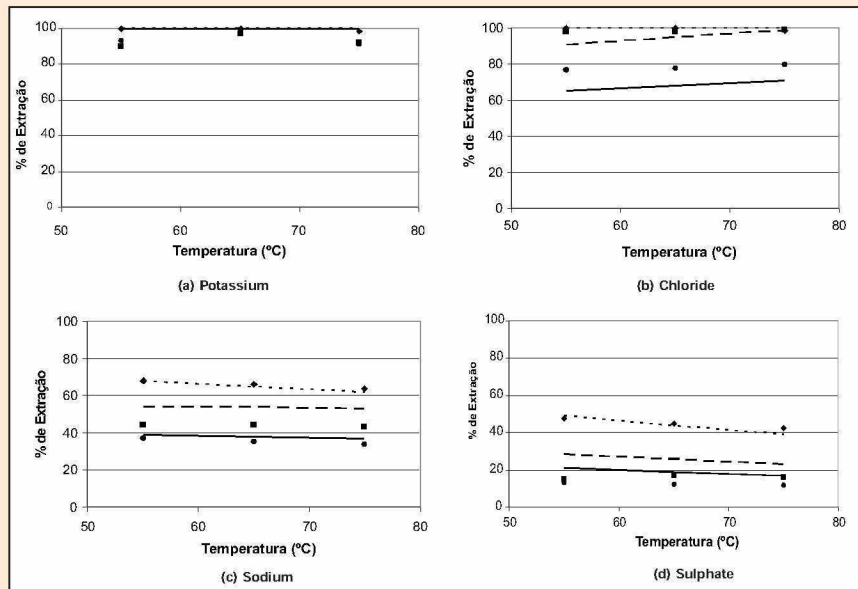


Figure 5 - Graphics of ions removal plotted versus temperature for Jaretun and Aly ash. Dotted line: model prediction of ash concentration equal to 0,6 kg/L

Dashed line: model prediction of ash concentration equal to 1,0 kg/L

Continuous line: model prediction of ash concentration equal to 1,4 kg/L

■ Experimental points of ash concentration equal to 0,6 kg/L

◆ Experimental points of ash concentration equal to 1,0 kg/L

● Experimental points of ash concentration equal to 1,4 kg/L

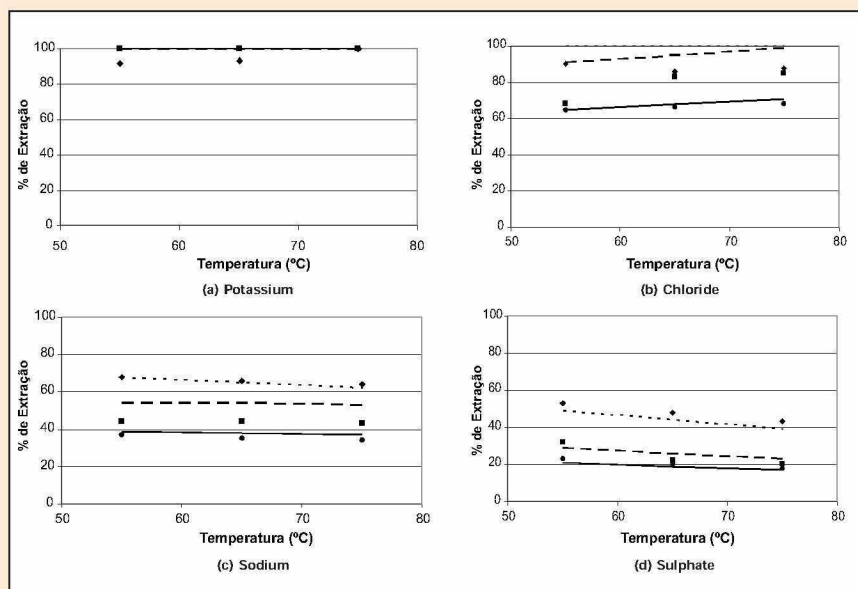


Figure 6 - Graphics of ions removal plotted versus temperature for synthetic ash.

Dotted line: model prediction of ash concentration equal to 0,6 kg/L

Dashed line: model prediction of ash concentration equal to 1,0 kg/L

Continuous line: model prediction of ash concentration equal to 1,4 kg/L

■ Experimental points of ash concentration equal to 0,6 kg/L

◆ Experimental points of ash concentration equal to 1,0 kg/L

● Experimental points of ash concentration equal to 1,4 Kg/L

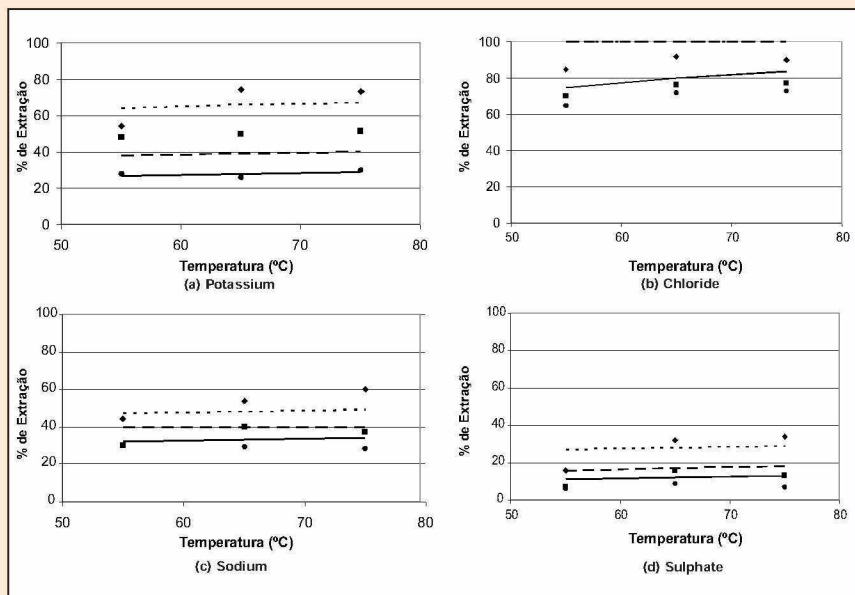


Figure 7 - Graphics of ions removal plotted versus temperature for industrial ash.

Dotted line: model prediction of ash concentration igual to 0,6 kg/L
 Dashed line: model prediction of ash concentration igual to 1,0 kg/L
 Continuous line: model prediction of ash concentration igual to 1,4 kg/L
 ■ Experimental points of ash concentration igual to 0,6 kg/L
 ◆ Experimental points of ash concentration igual to 1,0 kg/L
 ● Experimental points of ash concentration igual to 1,4 kg/L

dium sulphate, sodium chloride, and burkeite were identified in the solid phases of the synthetic ash and the compounds glasserite, sodium sulphate, sodium chloride and burkeite in those of the industrial ash. These results agree with predictions of Figure 1. It noteworthy to mention that it was impossible to identify the presence of sodium carbonate in the industrial ash solids because of interference between the peaks. In Table 7, it is showed a comparison of the extraction range predicted by the model with the experimental results found for these ions.

It can be observed in Table 6 and in Figures 5 and 6 that exits a good agreement between the range predicted for the removal and the experimental values. Also, it can be observed that the results obtained in Jaretun and Aly work are inside the predicted range. The synthetic ash of this work also shows a good agreement.

In Table 8 and in Figure 7 it can be observed comparisons between the experimental results and the range of extraction values calculated using the model for the industrial ash.

It is possible to verify that the chloride extraction is in accord to that expected. For carbonate, the situation is similar, but in this case, the extraction is superior to that expected. The sulphate results showed agreement between the model and experiments. Finally, sodium have a wider range, however only one point (60,2%) is located outside the predicted range.

The results of industrial ash have been used to verify the model efficiency in predicting the behaviour of ashes with different characteristics from the two previous synthetic materials. The formation of salts containing chloride and potassium after the leaching reduces the process efficiency. Therefore, the evaluation of the ash with different compositions allows to verify the model ability to predict formation of other salts, like glasserite, and also the behaviour of the leaching process. Accordingly to the thermodynamic model, the efficiency of this process will depend on the ash initial composition. For the industrial ash studied, the model could predict the glasserite formation, confirmed by the X-ray diffraction analysis, as well as the experimental extraction ranges, which show distinct behaviour from the synthetic ash. However, an analysis of the influence of the ash composition in the leaching process will be the goal of a forthcoming work.

CONCLUSIONS

Based on the phase diagram and the solubility curves determined by a thermodynamic model, it is determined the compounds formed in the solid phase, as well as the extraction le-

Table 8 - Extraction for ions: chloride, carbonate, sulphate and sodium for industrial ash

Ions	Extraction range predicted (%)	Extraction range of industrial ash (%)
Chloride	75 - 100	65 - 90
Carbonate	0	5 - 10
Sulphate	10 - 30	5 - 35
Sodium	32 - 50	30 - 60

vel of each ion (chloride, potassium, carbonate, sodium and sulphate) during the leaching of electrostatic precipitator ashes. Comparing the predicted values for each extraction with the experimental results, it has been observed a good agreement (differences not higher than 15%). Finally, with the purpose to verify the ash solid phase formation behaviour, X-ray diffraction analysis in the solid phase were made. The compounds predicted by the thermodynamic model were identified, which also contribute to turn reliable the use of the purposed model.

ACKNOWLEDGMENTS

This work was supported by "Fundação de Amparo a Pesquisa do Estado de Minas Gerais" (FAPEMIG/ BRAZIL) and "Conselho Nacional de Desenvolvimento Científico e Tecnológico" (CNPq/ BRAZIL).

LITERATURE

FERREIRA, L.M.A.; SOARES, M.A.R.; EGAS, A.P.V.; CASTRO, J.A.A.M.; Selective removals of chloride and potassium in kraft pulp mills; Tappi Journal; 2 (4): 63-66; 2003.

GILBERT, A.F.; The Effect of Potassium on the Effluent-Free Bleached Kraft Pulp Mill; PhD Thesis; Toronto University; 1976.

JARETUN, A.; ALY, G.; Leaching of chloride and potassium from precipitator catch; TAPPI International Chemical Recovery Conference; Vol. 3; 989-1008; Tampa; 1998.

JEMAA, N.; THOMPSON, R.; PALEOLOGOU, M.; BERRY, R.M.; Non-process elements in the kraft cycle, Part I : sources, levels and

process effects; Pulp and Paper Canada; 100 (9): 47-51; 1999.


JEMAA, N.; THOMPSON, R.; PALEOLOGOU, M.; BERRY, R.M.; Non-process elements in the kraft cycle, Part II : control and removal options; Pulp and Paper Canada; 101 (2): 41-56; 2000.

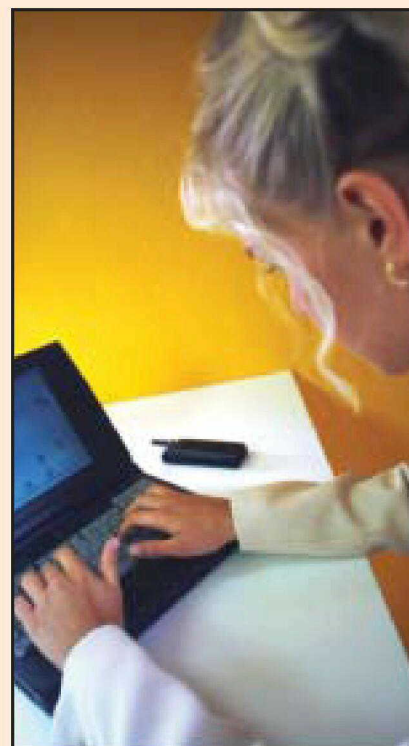
MALMBERG, B.; EDWARDS, L.; JÖNSSON, T.; THELANDIER, H.; SALTIN, J.; Dynamic modeling of potassium and chloride in the recovery area; Tappi Journal; 1 (4): 3-6; 2002.

MINDAY, A.M.; BURKE, M.A.; REID, D.W.; BROWN, C.J.; An overview of various strategies for balancing salt cake, chloride and potassium levels in an ECF kraft mill; TAPPI International Chemical Recovery Conference; Vol. 3; 961-970; Tampa; 1998.

PRYKE, D.C.; REEVE, D.W.; LUKES, J.A.; DONOVAN, D.A.; Valiquete, G.; Yemchuk, E.M.; Chemical recovery in the closed cycle mill / Part II: The salt recovery process; Pulp and Paper Canada; 84 (2): 59-62; 1983.

RICKETTS, J.; Considerations about the closed cycle mills; Tappi Journal; 77 (11): 43-49; 1994.

SATURNINO, D.M.; OLIVEIRA, E.D.; CARDOSO, M.; Redução dos Teores dos Íons Cloreto e Potássio na Unidade de Recuperação do Licor Negro das Indústrias de Papel e Celulose; Masters Dissertation; Federal University of Minas Gerais; Belo Horizonte, Brazil, 2003 (in portuguese). 



ABTCP and Uniscepa Informative Newsletters

Monthly electronic
newsletters that inform
you about ABTCP
activities and the most
recent research and
publications pertaining
to the industry.

Did you know that

... As an ABTCP member you are entitled to discounts when registering for events and can participate free of charge in Exhibitions organized by the Association? Find out more by contacting Vanessa Froiman at (55-11) 3874-2722, or Kellen Tonelli at (55-11) 3874-2735.